ChemComm

Accepted Manuscript

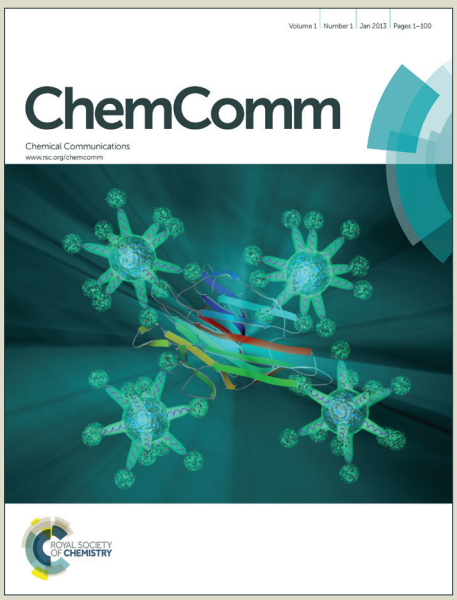

ROYAL SOCIETY OF CHEMISTRY

www.rsc.org/chemcomm

Diffusive fingering in a precipitation reaction driven by autocatalysis†

Eszter Tóth-Szeles,[a] Ágota Tóth,[a] and Dezső Horváth*[b]

Received Xth XXXXXXXXXX 20XX, Accepted Xth XXXXXXXXX 20XX
First published on the web Xth XXXXXXXXXX 200X
DOI: 10.1039/b000000x

The interaction of an autocatalytic reaction with a fast precipitation reaction is shown to produce a permanent precipitate pattern where the major driving force is differential diffusion. The final structure emerges from the leading transient cellular front, the cusps of which evolve into precipitate free zones. The experimental observations are reproduced by a simple model calculation based on the empirical rate-law of the reaction.

Chemical reactions far from the thermodynamical equilibrium may give rise to various types of self-organized spatiotemporal structures.[1,2] In distributed systems, the interaction between nonlinear chemical kinetics with transport processes may lead to the emergence of concentration and temperature gradients.[3,4] One of the simplest forms of spatial patterns is a chemical front due to the coupling of an autocatalytic reaction with diffusion.[5,6] The front is defined as a thin interface that spatially separates the reactants and the products of the reaction. A planar front propagating towards the homogeneously distributed reactants may become unstable if the flux of the reactant dominates over that of the autocatalyst, in which case the inherent noise is amplified to yield a structure with leading curved segments that are joined through sharp trailing cusps.[7–10] This cellular pattern only exists temporarily as a homogeneously distributed product solution will evolve eventually. Most emergent spatial patterns in homogeneous media are bound to be transient unless the system is kept far from equilibrium by some external input,[11] like Turing-patterns in an open reactor.[12]

Self-assembling permanent spatial chemical structures require a different approach. Carefully selected initial and boundary conditions have been successfully applied in designing precipitate patterns in various systems run in hydrogels where the symmetry of the final structure is a transformation of the original input.[13,14] Arbitrarily shaped Liesegang structures may be developed by controlling the coagulation threshold of the precipitation.[15]

In this work we combine the two aspects and construct a permanent spatial pattern, the symmetry of which emerges from the inherent instability of the homogeneous system. The coupling of an autocatalytic front with active transport has led to permanent structures in bacterium colonies as shown by Mimura[16,17]. Here we will demonstrate that the addition of a fast precipitation reaction to a reaction front exhibiting lateral instability is sufficient to fabricate permanent patterns.

We select the chlorite oxidation of tetrathionate for our model reaction, which is autocatalytic with respect to hydrogen ion.[18] Gelatine is added to the reactant mixture because its carboxylate groups will reversibly bind the autocatalyst providing the sufficient decrease in the flux of the free autocatalyst across the reaction front, a condition necessary for lateral instability.[19] In the presence of barium ions, the sulfate ions produced in the autocatalytic reaction yield precipitate via a fast reaction. The chemistry of the entire system can be summarized as

$$\begin{aligned} 7\,ClO_2^- + 2\,S_4O_6^{2-} + 6\,H_2O &\longrightarrow 7\,Cl^- + 8\,SO_4^{2-} + 12\,H^+ \\ M{-}COO^- + H^+ &\rightleftharpoons M{-}COOH \\ Ba^{2+} + SO_4^{2-} &\longrightarrow BaSO_4\downarrow \end{aligned} \qquad (1)$$

For small chlorite excess the empirical rate law for the autocatalysis has been formulated[20,21] as $r = k[ClO_2^-][S_4O_6^{2-}][H^+]^2$, which ensures the existence of a pushed-type reaction front as another condition necessary for lateral instability.[19]

Throughout the experiments reagent grade chemicals, with the exception of the technical grade sodium chlorite, were used with deionized water. Gelatine was dissolved in hot water and—when it cooled to room temperature—reactants were added to obtain solution with 5 mmol/L $K_2S_4O_6$, 20 mmol/L $NaClO_2$ and $Ba(NO_3)_2$, which, with 2.5–3.7 m/V% gelatine content, was then poured in a Hele-Shaw cell or a covered Petri dish to create a thin layer. After gelation a chemical front was initiated either by a short electrolysis at thin platinum wires stretched along the gel or by adding an acid drop at a specified point on the surface of the gel. The entire setup was thermostated at 17 or 4 °C. The front propagation was monitored by a CCD camera attached to a computer and the obtained images were evaluated by in-house softwares. In the precipitate-free control experiments bromophenol blue pH in-

† Electronic Supplementary Information (ESI) available. See DOI: 10.1039/b000000x/

[a] *Department of Physical Chemistry and Materials Science, University of Szeged, Szeged 6720, Hungary.*
[b] *Department of Applied and Environmental Chemistry, University of Szeged, Rerrich Béla tér 1, Szeged 6720, Hungary. E-mail: horvathd@chem.u-szeged.hu*

dicator (0.08 mmol/L) substituted barium nitrate.

Upon electrolysis, a reaction front is initiated at the anode, which then propagates at a constant velocity through the entire gel, while forming white barium sulfate precipitate behind the front. With gelatine content up to 2.5 m/V %, the planar reaction front is stable, the front therefore retains the geometry of the initiation (see Fig. 1(a,e)). At higher gelatine content, planar fronts become unstable giving rise to cellular reaction

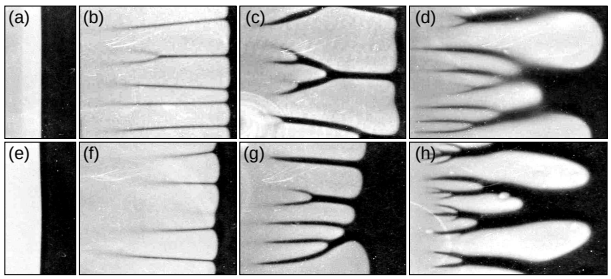

Fig. 1 White precipitate patterns with gelatine content 2.5 % (a,e) 2.7 % (b,f) 2.9 % (c,g) 3.33 % (d,h). Fronts propagate from left to right. Image height 43 mm. Time 1 h (a), 7 h (b), 18 h (c), 87 h (d), 40 min (e), 11 h (f), 24 h (g), 63 h (h) after initiation. Temperature 17 °C (a-d) and 4 °C (e-h)

fronts resembling patterns[22–24] emerged in viscous fingering. The distribution of the precipitate behind the front—shown in Fig. 1(b–d)—is not homogeneous: narrow precipitate free gaps (1–3 mm depending on the extent of binding) are created at the cusps of the leading autocatalytic front. Once formed, the entire precipitate pattern remains stationary, both the location and the width of the precipitate free zones appear independent of time as the reaction front invades the medium containing the reactant. This scenario is significantly different from that of the precipitate-free control experiments, where the produced autocatalyst finally takes on a homogeneous distribution. Comparison of the systems also reveals that the alignment of precipitate free gaps represents the trails left behind by the cusps of the autocatalytic reaction front.

Since gelatine is pH-sensitive, in experiments run at 17 °C, the pH decrease across the reaction is sufficiently large to cause the collapse of the gel structure, yielding the product system effectively in a sol state. It is important to point out that the gel structure is retained in the precipitate free gaps. The density of the solution varies with the change in composition, which may lead to fluid motion even though the product mixture is somewhat viscous and the thin medium is positioned horizontally. We have therefore repeated the experiments at 4 °C, at which temperature the gelatine remains in its gel form. As Fig. 1(e–h) shows, the same phenomenon can be observed: the onset of instability remains unchanged, above which the precipitate pattern with narrow precipitate free gaps emanating from the cusps of the cellular reaction evolves. This suggests that the underlying instability leading to the pattern formation has diffusive nature and the patterns only visually resemble to those of viscous fingering. The decrease in the velocity of propagation with increasing gelatine content listed in Table 1 supports the notion of diffusion-driven front instability. With more gelatine in the system, larger fraction of the

Table 1 Reaction front velocities (μm/s)

T(°C)	Gelatine content (m/V %)			
	2.5	2.7	2.9	3.33
4	9.28±0.46	1.25±0.04	0.583±0.003	0.171±0.003
17	15.70±0.70	2.00±0.15	0.770±0.008	0.184±0.002

hydrogen ion is bound to the matrix, leading to the decrease in the flux of the free autocatalyst across the front and eventually to the greater loss of planar front symmetry.

Having seen that convection has no contribution to the pattern formation, we can construct a reaction-diffusion model based on Eqs. (1). The reactant chlorite ion can be eliminated by considering the mass balance of Eqs. (1) and assuming the same diffusion coefficient for tetrathionate and chlorite ions. The dimensionless governing equations (for derivation see ESI†) take the form of

$$\frac{\partial \alpha}{\partial \tau} = \nabla^2 \alpha - \alpha\beta^2(\kappa + 7\alpha) \quad (2)$$

$$\sigma\frac{\partial \beta}{\partial \tau} = \delta\nabla^2 \beta + 6\alpha\beta^2(\kappa + 7\alpha) \quad (3)$$

$$\frac{\partial \gamma}{\partial \tau} = 4\alpha\beta^2(\kappa + 7\alpha) \quad (4)$$

where α, β, and γ are the relative concentration of $S_4O_6^{2-}$, H^+, and $BaSO_4$ precipitate with respect to $[S_4O_6^{2-}]_0$, while $\delta = D_{H^+}/D$ and $\kappa = 2[ClO_2^-]_0/[S_4O_6^{2-}]_0 - 7$. The temporal change in the total autocatalyst concentration in Eq. (3) can be given by introducing $\sigma = 1 + (K\mu)/(K+\beta)^2$, where K is the dimensionless dissociation constant of the fast protonation in Eq. (1) and μ is the relative total concentration of carboxylate groups in the gel. The absence of the diffusion term in Eq. (4) corresponds to the formation of the immobile precipitate. Equations (2–4) are solved by an explicit Euler method on a square grid with a spacing of 0.4 and a time step of 10^{-3}.

Figure 2 summarizes the obtained precipitate patterns for various gelatine content and diffusion coefficient ratio. The former is selected to match the experiments presented in Fig. 1 above the onset of lateral instability ($\mu = 4.8$ corresponds to 2.7 % gelatine content), while the latter is used because the exact diffusion coefficients of the species are unknown. In all cases the propagating reaction front leaves behind the precipitate pattern. While from the homogeneous distribution of reactants the reaction front builds up a homogeneous distribution of autocatalyst sufficiently far behind, the resultant precipitate pattern remains structural. The precipitate lean narrow gaps emanate from the cusps of the generating reaction front similarly to those seen in the experiments. In the vicinity of the cusps the flux of reactant is less than at the leading edge of the front due to the curvature, hence less product is formed.

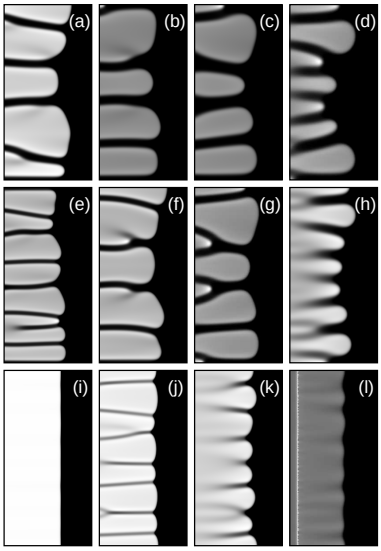

Fig. 2 Calculated precipitate patterns formed behind the reaction front propagating from left to right with μ 4.4 (a,e,i) 4.8 (b,f,j) 5.2 (c,g,k) 5.6 (d,h,l). Ratio of diffusion coefficients (δ) 0.5 (a-d) 1 (e-h) 2 (i-l) and image height 45 mm

This decrease in concentration is amplified by the presence of a consecutive reaction producing an immobile species, barium sulfate in this case. While the autocatalyst slowly fills up the gaps by diffusion as the front propagates on, the amount of precipitate remains very low in these narrow region marking the location of the cusps.

The local depletion of the reactants leads to the formation of precipitate lean narrow regions not only right behind the cusps but also when reaction fronts annihilate upon collision as shown in Fig. 3, where the final precipitate pattern is shown after the reactant is completely consumed. The model calculation reproduces the experimental observation remarkable well: in Fig. 3 the size of the calculation domain matches the physical size of the experimental image without fitting parameters, at the same time there is quantitative agreement in the width of the precipitate lean gaps (see ESI†).

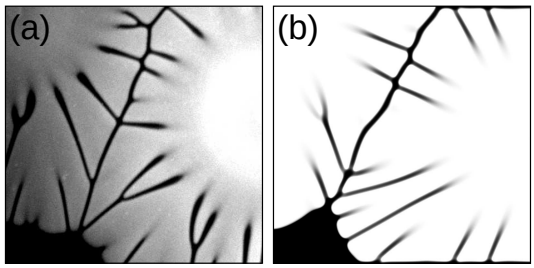

Fig. 3 Precipitate pattern behind the annihilation of two reaction front. Experimental image with 8 cm width (a), calculated pattern with 9 cm width (b)

In this work we have shown that a consecutive reaction producing an immobile species can be used to generate a final stable pattern from the transient spatial pattern of an autocatalytic reaction front. Here a precipitate reaction is utilized but the experiments have revealed that the proper selection of the polymer hydrogel can also be of use with a gel-sol transition initialized by the autocatalysis. The cusps generally exhibit transverse motion in the front therefore the precipitate free gaps emanating from them result in intricate patterns. By running the reaction in a confined space one may stabilize the cusps in which case more symmetric final pattern can be manufactured. This method may then represent a novel approach in the synthesis of self-organized materials with spatial gradients.

The work was supported by the Hungarian Research Fund (OTKA K72365) and TÁMOP-4.2.2.A-11/1/KONV-2012-0047.

References

1 C. Kapral and K. Showalter, *Chemical Patterns and Waves*, Kluwer, Dordrecht, 1995.
2 I. R. Epstein and J. A. Pojman, *An Introduction to Nonlinear Chemical Dynamics*, Oxford University Press, Oxford, 1998.
3 A. Hagberg and E. Meron, *Phys. Rev. E*, 1993, **48**, 705.
4 J. E. Pearson, *Science*, 1993, **261**, 189.
5 L. Szirovicza, I. Nagypál and E. Boga, *J. Am. Chem. Soc.*, 1989, **111**, 2842.
6 P. Gray and S. K. Scott, *Chemical Oscillations and Instabilities*, Claridon Press, Oxford, 1990.
7 G. I. Sivashinsky, *Combust. Sci. Technol.*, 1977, **15**, 137.
8 Y. Kuramoto, in *Dynamics of Synergetic Systems*, Springer, Berlin, 1980, p. 134.
9 D. Horváth, V. Petrov, S. K. Scott and K. Showalter, *J. Chem. Phys.*, 1993, **98**, 6332.
10 D. Horváth and K. Showalter, *J. Chem. Phys.*, 1995, **102**, 2471.
11 Q. Ouyang and H. L. Swinney, *Nature*, 1990, **352**, 610.
12 J. Horváth, I. Szalai and P. D. Kepper, *Science*, 2009, **324**, 772.
13 I. T. Bensemann, M. Fialkowski and B. A. Grzybowski, *J. Phys. Chem. B*, 2005, **109**, 2774.
14 B. A. Grzybowski, *Chemistry in Motion*, Wiley, Chichester, 2009.
15 F. Molnár, F. Izsák and I. Lagzi, *Phys. Chem. Chem. Phys.*, 2008, **10**, 2368.
16 M. Mimura, H. Sakaguchi and M. Matsushita, *Physica A*, 2000, **282**, 283.
17 A. Aotani, M. Mimura and T. Mollee, *Japan J. Indust. Appl. Math.*, 2010, **27**, 5.
18 A. Tóth, I. Lagzi and D. Horváth, *J. Phys. Chem.*, 1996, **100**, 14837.
19 D. Horváth and A. Tóth, *J. Chem. Phys.*, 1998, **108**, 1447.
20 I. Nagypál and I. R. Epstein, *J. Phys. Chem.*, 1986, **90**, 6285.
21 A. K. Horváth, I. Nagypál and I. R. Epstein, *Inorg. Chem.*, 2006, **45**, 9877.
22 A. De Wit and G. M. Homsy, *J. Chem. Phys.*, 1999, **110**, 8663.
23 T. Gérard and A. De Wit, *Phys. Rev. E*, 2009, **79**, 016308.
24 D. Bonn, H. Kellay, M. Bräunlich, M. Ben Amar and J. Meunier, *Physica A*, 1995, **220**, 60.